

# Prostate Cancer localization with a Multiparametric MR Approach (PCaMAP): separating PCa from benign tissue in a multi-center study

Marnix C. Maas<sup>1</sup>, Alan J. Wright<sup>1</sup>, Kirsten M. Selnæs<sup>2,3</sup>, Masoom A. Haider<sup>4</sup>, Katarzyna J. Macura<sup>5</sup>, Daniel J.A. Margolis<sup>6</sup>, Berthold Kiefer<sup>7</sup>, Jurgen J. Fütterer<sup>1</sup>, and Tom W.J. Scheenen<sup>1</sup>

<sup>1</sup>Radiology, Radboud University Medical Center, Nijmegen, Netherlands, <sup>2</sup>Department of Circulation and Medical Imaging, Norwegian University of Science and Technology, Trondheim, Norway, <sup>3</sup>St. Olavs Hospital, Trondheim University Hospital, Trondheim, Norway, <sup>4</sup>Sunnybrook Health Sciences Centre, University of Toronto, Toronto, Ontario, Canada, <sup>5</sup>Russell H. Morgan Department of Radiology and Radiological Science, Johns Hopkins University, Baltimore, MD, United States, <sup>6</sup>UCLA David Geffen School of Medicine, Los Angeles, CA, United States, <sup>7</sup>Siemens AG Healthcare Sector, Erlangen, Germany

## Introduction

PCaMAP (NCT01138527) aims to prove the diagnostic accuracy of multi-parametric MR imaging (mpMRI) at 3T without an endorectal coil (ERC) in a multi-center setting for distinguishing clinically significant prostate cancer from other prostate tissue, with whole-mount section histopathology of resected prostates as the gold standard. The measurement protocol comprised three functional imaging techniques in addition to high resolution T<sub>2</sub>-weighted imaging: diffusion weighted imaging (DWI), dynamic contrast enhanced (DCE) imaging and <sup>1</sup>H-spectroscopic imaging (MRSI). Here we present initial results of the validation part of this study.

## Methods

Fifty patients from 5 institutions (12, 10, 10, 10 and 8 patients) were included (mean±SD age 61±7y, PSA 7.4±3.5 ng/ml, Gleason score [GS] range 5-9). All centers used identical scanning protocols on 3T MRI systems (Siemens Healthcare, Erlangen) using external body and spine array coils. High-resolution T<sub>2</sub>-weighted imaging was performed in three orthogonal directions. DWI was acquired with *b*-values of 0, 100, 400, 800 s/mm<sup>2</sup>, and ADC maps were calculated. 3D MRSI was performed with a PRESS sequence (TR/TE 750/145 ms). Spectra were automatically quality checked (QC)<sup>1</sup> and fitted accounting for contributions of choline (Cho), spermine (Spm), creatine (Cr) and citrate (Ci) using LCModel<sup>2</sup>. DCE data were acquired using a T<sub>1</sub>-weighted TWIST sequence (time resolution 4s) and processed using a two-compartment Tofts model (Tissue4D, Siemens Healthcare) with a population based arterial input function (AIF), yielding maps of K<sup>trans</sup>, k<sub>ep</sub>, v<sub>e</sub>, and the initial area under the enhancement curve (iAUC). Tumors were individually outlined and graded on histology slides according to a study-specific protocol<sup>3</sup>. Guided by histopathology and blinded to any functional MR data, a spectroscopist in consensus with an experienced radiologist selected non-neighboring MRSI voxels in non-cancer peripheral zone (PZ), non-cancer combined transition and central zone (CG), and prostate cancer (PCa, volume >0.5 cc) as regions of interest (ROIs)<sup>4</sup>. A sphere of the approximate true size of an MRSI voxel (1.0 cc) was placed on each selected MRSI voxel to extract imaging parameters at the corresponding locations. Spheres were trimmed so as to contain only the tissue of interest (Fig 1). As the most characteristic value of the various quantities may occur at different locations within the same tumor, a maximum of 6 neighboring, overlapping MRSI voxels directly adjacent to the original voxel in 3 dimensions were included as additional representative ROIs (Fig. 1), provided they were located in the same tissue<sup>4</sup>. For each sphere the following quantities were calculated: 25<sup>th</sup> percentile (25p) for ADC, 75p for K<sup>trans</sup>, k<sub>ep</sub> and iAUC, and 50p for v<sub>e</sub>. The most deviating value of each parameter in each ROI group was used for further analysis.

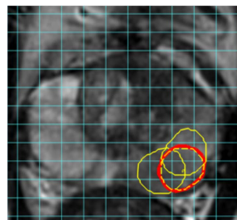


Fig. 1: ROI groups consisted of a central ROI (red) and its direct neighbours (yellow) in 3 directions (maximum 6). The dashed sphere is located superior to the central ROI. In this example of non-cancer PZ the ROIs to the right and posterior to the central voxel fall outside the prostate and are excluded from analysis.

## Results

A total of 70 tumors >0.5cc indicated on histopathology were annotated (GS<6: 2, GS 3+3=6: 19, secondary or tertiary GG 4 and no GG 5: 23, primary GG 4 or any GG 5: 21, and unknown GS: 5). 54 tumors originated from the PZ, and 16 tumors from the CG. 1756 ROIs were annotated (349 original, 1407 neighbors), of which 712 (136 original) were in prostate cancer. Automatic QC passed 53% of MRSI voxels (worst-performing center 28%, best-performing center 68%). Significant differences between non-cancer PZ and PCa were found for ADC (Fig. 2), (Choline+Spermine+Creatine)/Citrate [CSC/C], Choline/(Spermine+Creatine) [C/SC], K<sup>trans</sup> and v<sub>e</sub> (all *p*<0.001). Significant differences between non-cancer CG and PCa were found for ADC (*p*<0.001) and C/SC (*p*<0.05). ROC analysis resulted in AUC comparable to literature values for ADC (Table 1), but lower than previously published values for MRSI and DCE parameters<sup>5,6</sup>. A Logistic Regression Model (LRM) including ADC, CSC/C and K<sup>trans</sup> did not yield an improvement over using ADC alone.

## Discussion

The approach of including multiple MRSI voxels per ROI reduced inaccuracy of spatial matching between histopathology slides and MRI. Using the most deviating voxel of each quantity in each original ROI with adjacent neighbors in both cancerous and non-cancer tissues avoided biasing the analysis. The ADC results indicate that this method can yield similarly good separation between the various tissue types as found in existing literature, while allowing for combining imaging modalities with strongly different spatial resolutions. Other parameters, especially those derived from DCE, showed poorer results than literature values. It is unlikely that this is due to variations in parameter values between the different centers<sup>7</sup>. Employing individualized AIFs or using tissue calibration may improve DCE-based separation. Acquiring MRSI data without an ERC and varying levels of local experience contributed to the relatively low number of voxels passing the automated QC procedure, reducing the amount of data usable for separating tissue types. Existing methods for combining various metabolite ratios still need to be adapted to the explicit inclusion of spermine in the fitting procedure<sup>8</sup>. Although histologic differences between TZ and PZ tumors exist, no distinction between these tumor types could be made in this study owing to the low number of TZ tumors.

## Conclusions

Using identical scanning protocols at 3T without an ERC in a multi-center setting yields good separation of PCa tissue from non-cancer tissues with ADC maps. Data analysis of DCE and MRSI needs further steps before definite conclusions about the multi-center performance of these methods can be drawn. The validation part of this prospective trial will be used to determine the parameters contributing most to the detection and localization of clinically significant PCa as well as their optimal threshold values.

## References

<sup>1</sup>Wright, *NMR Biomed* 26:193–203 (2013); <sup>2</sup>Provencher, *Magn Reson Med* 30:672–79 (1993); <sup>3</sup>Epstein, *Am J Surg Pathol* 29:1228–42 (2005); <sup>4</sup>Scheenen, *Invest Radiol* 46:25–33 (2011); <sup>5</sup>Selnæs, *Invest Radiol* 47:624–33 (2012); <sup>6</sup>Ocak, *Am J Roentgenol* 189:W192–W201 (2007); <sup>7</sup>Maas, *ISMRM* 2013 (#1769); <sup>8</sup>Fütterer, *Invest Radiol* 42:116–22 (2007).

**Acknowledgements:** ERC Grant agreement n° [243115], Siemens Healthcare for research support, the PCaMAP consortium for collaborative support.

Table 1: Areas under the ROC curve of DWI, DCE and MRSI-derived parameters for separating PCa from non-cancer PZ, non-cancer CG, and both non-cancer tissues. 95% confidence limits were all  $\leq \pm 0.11$  around the mean.

	PZ	CG	Both
ADC	0.88	0.71	0.78
CSC/C	0.73	0.64	0.68
C/SC	0.70	0.64	0.67
K <sup>trans</sup>	0.67	0.56	0.62
LRM	0.89	0.72	0.81

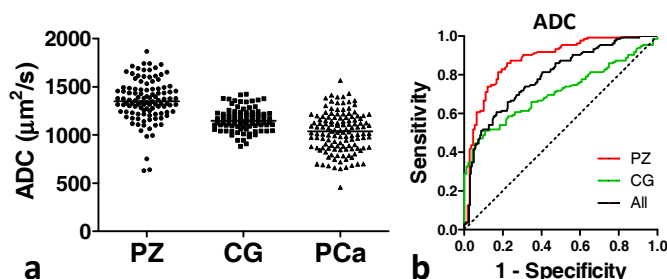


Fig. 2: a: Minimum of 25<sup>th</sup> percentiles of ADC values found in each ROI group for non-cancer PZ, non-cancer GG and PCa. All differences were *p*<0.001. b: ROC curves for PCa vs non-cancer PZ (red), PCa vs non-cancer CG (green) and PCa vs all non-cancer tissue (black).